Experimental Gerontology 206 (2025) 112782

Contents lists available at ScienceDirect

Experimental Gerontology

journal homepage: www.elsevier.com/locate/expgero

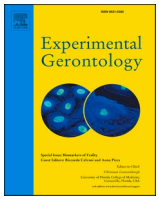

Association between diffusion MRI-based measures of neurite microstructure and risk of Alzheimer's disease

Sasha Hakhu, Andrew Hooyman, Jennapher Lingo VanGilder, Sydney Y. Schaefer, Scott C. Beeman *, Alzheimer's Disease Neuroimaging Initiative[1]

School of Biological and Health Systems Engineering, Arizona State University, 550 E Orange St., Tempe, AZ 85287, United States of America

ARTICLE INFO

Section Editor: Tibor Hortobagyi

Keywords:
AD
APOE-e4
Diffusion MRI
NODDI

ABSTRACT

Early detection of Alzheimer's disease (AD) is crucial for intervention, but traditional MRI and cognitive assessments may miss pre-symptomatic changes. Advanced diffusion MRI (dMRI) methods, such as Neurite Orientation Dispersion and Density Imaging (NODDI), show promise in identifying early brain changes. We analyzed 65 cognitively unimpaired older adults (25 APOE-e4 carriers, 40 non-carriers) from the ADNI3 dataset. NODDI's neurite density index (NDI) and orientation dispersion index (ODI), volumetric MRI and cognition (MoCA) were analyzed in key brain regions like the hippocampus, fusiform gyrus, and entorhinal cortex. Statistical analyses included linear regression and *t*-tests, with FDR correction. NDI differed significantly between carriers and non-carriers and correlated with MoCA scores. ODI differed only in the CA1 hippocampal subfield. Volumetric MRI measures showed no group differences. Significant APOE-e4 group differences were observed in NDI for the left fusiform gyrus ($\beta = 0.015$, $p = 0.02$), right fusiform gyrus ($\beta = 0.018$, $p = 0.02$), left entorhinal cortex ($\beta = 0.018$, $p = 0.04$), right entorhinal cortex ($\beta = 0.018$, $p = 0.03$), left CA1 ($\beta = 0.03$, $p = 0.02$), and left CA2–3 ($\beta = 0.03$, $p = 0.02$). ODI differences were observed only in left CA1 ($\beta = 0.037$, $p = 0.008$). No volumetric measures differed significantly. MoCA correlated with NDI in bilateral entorhinal cortices ($p = 0.001$–0.05), left fusiform gyrus ($p = 0.02$), and right CA2–3 ($p = 0.02$). NODDI metrics, particularly NDI, could help detect early APOE-e4-related microstructural changes, while traditional volumetric MRI measures remain uninformative at early stages.

1. Introduction

Early disease identification and intervention are critical for treating Alzheimer's disease (AD). Therapies targeting amyloid and tau slow disease progression, potentially extending the patient's quality of life (Zhang et al., 2023); however, these treatments are most effective earlier on (Albert et al., 2002). Advances in imaging techniques have significantly enhanced our ability to detect changes leading up to AD. Positron emission tomography (PET) uses radiotracers to measure AD-linked abnormalities like glucose metabolism (Landau et al., 2011; Reiman et al., 2001), amyloid plaque deposition and tau neurofibrillary tangles (Nordberg et al., 2010; Saint-Aubert et al., 2017; Mak et al., 2024). Amyloid-PET visualizes plaques, which disrupt neuronal communication and trigger inflammation, leading to neurodegeneration before cognitive decline (Nordberg et al., 2010). Tau-PET tracks tau tangles that disrupt neuronal transport systems, resulting in cell death (Saint-Aubert et al., 2017). Other tools such as neuropsychological assessments, blood biomarkers, and structural magnetic resonance imaging (MRI) can monitor symptoms and pathology (Nordberg et al., 2010; Mukherji et al., 2022; Albert et al., 2001; Frisoni et al., 2010); but only reflect macroscopic changes occurring *after* cognitive deficits. They fail to capture subtle, early microstructural alterations in brain tissue preceding neurodegeneration and symptom onset. A non-invasive method is needed to directly measure neurodegeneration by quantifying actual neuronal degradation characteristic of neurodegenerative diseases like AD.

Diffusion magnetic resonance imaging (dMRI) offers an avenue for early and accurate AD screening (Goveas et al., 2015) by detecting

* Corresponding author at: 550 E Orange St., Tempe, AZ 85287, United States of America.
E-mail address: Scott.Beeman@asu.edu (S.C. Beeman).

[1] Data used in preparation of this article were obtained from the Alzheimer's Disease Neuroimaging Initiative (ADNI) database (adni.loni.usc.edu). As such, the investigators within the ADNI contributed to the design and implementation of ADNI and/or provided data but did not participate in analysis or writing of this report. A complete listing of ADNI investigators can be found at: http://adni.loni.usc.edu/wp-content/uploads/how_to_apply/ADNI_Acknowledgement_List.pdf.

https://doi.org/10.1016/j.exger.2025.112782
Received 11 November 2024; Received in revised form 7 May 2025; Accepted 12 May 2025
Available online 14 May 2025
0531-5565/© 2025 The Authors. Published by Elsevier Inc. This is an open access article under the CC BY license (http://creativecommons.org/licenses/by/4.0/).

microstructural changes (Douaud et al., 2013; Hoy et al., 2017; Zhuang et al., 2013) that precede symptomatic AD. Although dMRI itself is not a novel technique, recent advancements in acquisition protocols and biophysical modelling have dramatically expanded its utility in quantification of neuropathological processes (Kamiya et al., 2020), particularly those involving neurodegeneration (Kamiya et al., 2020; Wen et al., 2015). dMRI non-invasively measures the diffusion-driven displacement of water in spaces like intra/extra-cellular spaces and neurites to infer tissue microstructural features quantitively (e.g., cell size or neurite density) (Tournier, 2019); thus capturing diffusion patterns reflecting underlying structures. For example, water in white matter moves freely axially but is restricted radially, producing anisotropy. In gray matter, diffusion is more uniform thus creating isotropic patterns. Multi-shell dMRI captures varied tissue microenvironments, and biophysical models quantify diffusion corresponding to microstructure (e.g., neurite density/orientation). It provides a non-invasive, repeatable method for distinguishing between pathological and healthy tissue microstructure, with applications in detecting AD (Yu et al., 2024; Xu et al., 2000). Specifically, neurite orientation dispersion and density imaging (NODDI) (Zhang et al., 2012) models the diffusion signal by compartmentalizing volume fractions into “free water,” “intra-neurite,” and “extra-neurite” spaces. NODDI quantifies neurite structural integrity, where higher neurite density index (NDI) values indicate greater neurite density, and lower orientation dispersion index (ODI) values reflect greater coherence.

The APOE-e4 allele increases AD risk (Abraham et al., 2020; Caselli et al., 2004) for early- and late-onset cases. (van Duijn et al., 1994; Locke et al., 1995) Studies show strong correlations between structural degradation and APOE-e4 (Mak et al., 2024; Evans et al., 2020; Du et al., 2021) suggesting neurite density loss may be an early marker of disease pathology. (Mak et al., 2024; Evans et al., 2020; Du et al., 2021; Montal et al., 2018; Slattery et al., 2017; Burggren and Brown, 2014) PET imaging detects amyloid plaques (Nordberg et al., 2010) and tau proteins (Nordberg et al., 2010; Mak et al., 2023), important biomarkers of AD. However, due to its high costs, limited availability, reliance on radioactive tracers, and lack of direct reporting on actual neurodegeneration (loss of cell bodies and/or neurites), other non-invasive methods for early detection and monitoring of neurodegeneration are needed. dMRI is non-invasive, accessible, cost-effective and provides a direct measure of neurodegeneration based on microstructural measures, making it complementary to plasma biomarkers for early detection, especially in pre-symptomatic individuals.

We tested whether dMRI-measured neurite structural integrity was lower in cognitively unimpaired APOE-e4 carriers than non-carriers. Neuroimaging data from the Alzheimer's Disease Neuroimaging Initiative (ADNI) database (adni.loni.usc.edu) were analyzed using NODDI-derived NDI and ODI calculated in prospectively-identified regions of interest, including the fusiform gyrus, entorhinal cortex, and hippocampal subfields (cornu ammonis CA1, CA2-3) (Twamley et al., 2006; Devanand et al., 2012; Malek-Ahmadi et al., 2023; Hamza et al., 2022; Jessen et al., 2006; Ma et al., 2020). NODDI-based metrics were correlated with the Montreal Cognitive Assessment (MoCA). Standard volumetric MRI measures were evaluated to determine whether diffusion metrics offered unique insights. We hypothesized that APOE-e4 carriers would have lower NDI (i.e., reduced neurite density) and higher ODI (i.e., increased neurite dispersion) values in the fusiform gyrus, entorhinal cortex, and hippocampal subfields than non-carriers. Given the greater significance of left hemispheric hippocampal changes in AD development (Caselli et al., 2004; Jessen et al., 2006), we hypothesized lower NDI and higher ODI values in the left hemisphere of carriers. Lastly, we hypothesized that MoCA scores would significantly correlate with dMRI-based metrics, but not with standard T1-based volume measures, given that microstructural changes like alterations in neurite density and orientation dispersion, likely occur much earlier in the disease process before substantial volume loss is apparent (Douaud et al., 2013; Hoy et al., 2017; Zhuang et al., 2013).

2. Methods

2.1. Participants

Sixty-five cognitively unimpaired older adults were analyzed in this study to obtain brain dMRI and neuropsychological testing data. Mean age overall was 69.5 ± 5.5 years (range = 62 to 90 years; 45 females). The dataset used in preparation of this study was obtained from the Alzheimer's Disease Neuroimaging Initiative (ADNI3, 2017) (Weiner et al., 2017) database (adni.loni.usc.edu), consisting of cognitively unimpaired APOE-e4 carriers (n = 25, including 3 homozygotes) and non-carriers (n = 40). ‘Carriers’ were defined as having a least one e4 allele. The carrier and non-carrier groups were not significantly different in terms of age ($p = 0.22$). To evaluate statistical power, we conducted both a priori and *post-hoc* power analyses. A priori power analyses indicated that approximately 64 participants per group would be required to detect a medium effect size (Cohen's $d = 0.5$) with 80 % power at $\alpha = 0.05$. Given our actual group sizes (carriers, e4+ n = 25 and non-carriers, e4− n = 40), we performed a post-hoc power analysis using an observed effect size of $d = 0.67$, which yielded a power of approximately 73.5 %. This suggests that our study was sufficiently powered to detect moderate-to-large effects in key regions, though underpowered to reliably detect smaller effects.

2.2. Neuroimaging data acquisition

Data used in the preparation of this article were obtained from the Alzheimer's Disease Neuroimaging Initiative (ADNI) database (adni.loni.usc.edu). The ADNI was launched in 2003 as a public-private partnership, led by Principal Investigator Michael W. Weiner, MD. The primary goal of ADNI has been to test whether serial magnetic resonance imaging (MRI), positron emission tomography (PET), other biological markers, and clinical and neuropsychological assessment can be combined to measure the progression of mild cognitive impairment (MCI) and early Alzheimer's disease (AD).

Data used in this study were acquired using the ADNI-3 advanced protocol (Weiner et al., 2017) on a 3 T scanner. All scans used in this study were acquired using 3 T Siemens scanners, consistent with the ADNI3 protocol. The electronic sequences used were provided by the Mayo Clinic Alzheimer's Disease Imaging Research (ADIR) group (ADNI, n.d.-a). The following data were processed in this study: (i) MPRAGE T1-w image (TR = 2300 ms, TI = 900 ms) and (ii) multi-shell diffusion data with three shells: b = 500, 1000, 2000 s/mm^2 (TR/TE 3300/71 ms, 112 total diffusion weighted directions) and thirteen interleaved b = 0 s/mm^2 values. Our analysis was limited to Siemens 3 T scanners using harmonized ADNI3 imaging protocols to minimize inter-site variability. All ADNI3 T1 images include an on-scanner non-uniformity correction. Additionally, we have performed the following data processing steps to account for bias field and motion distortion correction (ADNI, n.d.-b).

2.3. Neuroimaging data processing

Data were pre-processed using FSL (Jenkinson et al., 2012) and MRtrix (Tournier et al., 2019). The raw diffusion data underwent noise correction, susceptibility distortion correction (Synb0 (Schilling et al., 2019)), motion and eddy current-induced distortion correction (Andersson and Sotiropoulos, 2016) and bias field correction.

The NODDI model was then applied to the diffusion data (MATLAB toolbox (Microstructure Imaging Group, n.d.)) to obtain neurite density index (NDI) and orientation dispersion index (ODI), which are both scaled from 0 to 1. NDI is a measure of neurite volume fraction (a value of 1 suggesting a denser population of neurites), while ODI is a measure of neurite coherence (a value of 1 suggesting greater dispersion of neurites). Functionally speaking, NDI reflects the density of neurite packing while ODI reflects the degree of aligned or scattered neurites in space.

Following this, brain-extracted T1 and b0 images underwent linear image co-registration (Jenkinson et al., 2002), followed by a non-linear transformation (Andersson, n.d.) to the Montreal Neurological Institute (MNI) standard brain atlas (https://www.bic.mni.mcgill.ca/ServicesAtlases/HomePage, n.d.). For this study specifically, regions-of-interest (ROIs) were acquired from the Harvard-Oxford cortical and subcortical structural atlases (Desikan et al., 2006) and non-linearly transformed to an older brain atlas (Gordon et al., 2015) (to address issues such as age-related ventricular displacement, etc.). Hippocampal subfields were obtained using the Juelich Histological atlas (also in standard MNI space) (Amunts et al., 2005). ROI-based mean values and standard deviations for NDI and ODI were extracted and analyzed. These regions of interest (fusiform gyrus, entorhinal cortex and hippocampal subfields) were selected a priori based on previous demonstration of their crucial role in memory and other cognitive functions (Twamley et al., 2006; Devanand et al., 2012; Malek-Ahmadi et al., 2023; Hamza et al., 2022; Jessen et al., 2006; Ma et al., 2020; Yetkin et al., 2006; Berghuis et al., 2019; Bo and Seidler, 2009; Langan and Seidler, 2011).

Additionally, standard volumetric calculations were calculated by using these segmented brain ROIs, overlaying them onto T1-weighted images, extracting the volume measures for each region (using FSL), and then comparing the volumetric differences between carriers and non-carriers. Each ROI underwent non-linear warping and co-registration to the native space of each participant. This approach inherently accounts for individual differences in brain size and morphology, ensuring that volumetric measures reflect region-specific characteristics relative to each brain's anatomy.

2.4. Cognitive assessment

Scores from the Montreal Cognitive Assessment (MoCA) (Weiner et al., 2017) were also analyzed for the participants included in this study. Although the participants were classified as cognitively unimpaired within the ADNI dataset based on extensive neuropsychological evaluation, examining MoCA scores allowed for the investigation of potential associations between global cognitive scores, APOE-e4 carrier status, and microstructural changes at the neurite level.

2.5. Statistical analysis

Statistical analyses were performed using R version 4.2.2 (*R: The R Project for Statistical Computing*, n.d.). Linear regression models were employed to compare NDI, ODI, and volumetric measurements in the left (L) and right (R) hemispheric regions of the brain between APOE-e4 carrier and non-carrier groups. Brain regions analyzed included the fusiform gyrus, entorhinal cortex, and hippocampal subfields (cornu ammonis CA1, CA2-3, CA4). The focus on hippocampal subfields is justified due to their established association with AD (Xu et al., 2000; Killiany et al., 2002; Rao et al., 2022; Pennanen et al., 2004). By analysing the left and right regions individually rather than looking at them as a summed total, we aimed to capture lateralized effects that may be relevant to the pathology (Abraham et al., 2020; Jessen et al., 2006; Mohtasib et al., 2022; Baxter et al., 2023). ROIs were spatially normalized through warping and co-registration (in the preprocessing steps) to align template ROI masks to each participant's coordinate space and address individual differences in brain size and shape.

A linear regression model was used to examine the effect of APOE-e4 status on various brain region metrics. APOE-e4 status (carrier vs. non-carrier) was modelled as the independent variable, while the mean NDI and volume values of different ROIs and cognitive scores (MoCA) were treated as dependent variables. To assess the significance of the differences between the carrier and non-carrier groups, *t*-tests were performed between MRI metrics for each region and cognitive score between groups. A false discovery rate (FDR) correction step was applied to account for multiple comparisons. Box plots and scatter plots were generated to visualize the differences between the groups. Statistical significance was set at $p \leq 0.05$.

Additionally, because MoCA scores did not vary based on carrier status (see Results), groups were collapsed across carrier status to evaluate the extent to which MoCA scores varied as a function of NDI and ODI values and standard volumetric measures in specific regions of interest. We examined the sensitivity of these diffusion metrics relative to volumetric methods based on cognitive measures and APOE-e4 status. Volumetric and NDI measures were standardized to z-scores for comparison, and linear regression models were used to analyse how measurements of brain regions, such as NDI and volume, affect MoCA scores, while controlling for age and sex.

3. Results

Figs. 1, 2 and 3 show NDI, ODI, and standard volumetric calculations respectively, for the left and right regions of interest. Region-specific results and participant demographics are summarized in Table 1. Results demonstrated a significant effect of APOE-e4 carrier status (carrier vs. non-carrier) on NDI values in the left fusiform gyrus ($\beta = 0.015$, 95 % CI = [0.002; 0.02], $p = 0.02$), right fusiform gyrus ($\beta = 0.018$, 95 % CI = [0.003; 0.03], $p = 0.02$) (Fig. 1a), left entorhinal cortex ($\beta = 0.018$, 95 % CI = [0.002; 0.03], $p = 0.04$) and right entorhinal cortex ($\beta = 0.018$, 95 % CI = [0.001; 0.03], $p = 0.03$) (Fig. 1b). Furthermore, NDI values were

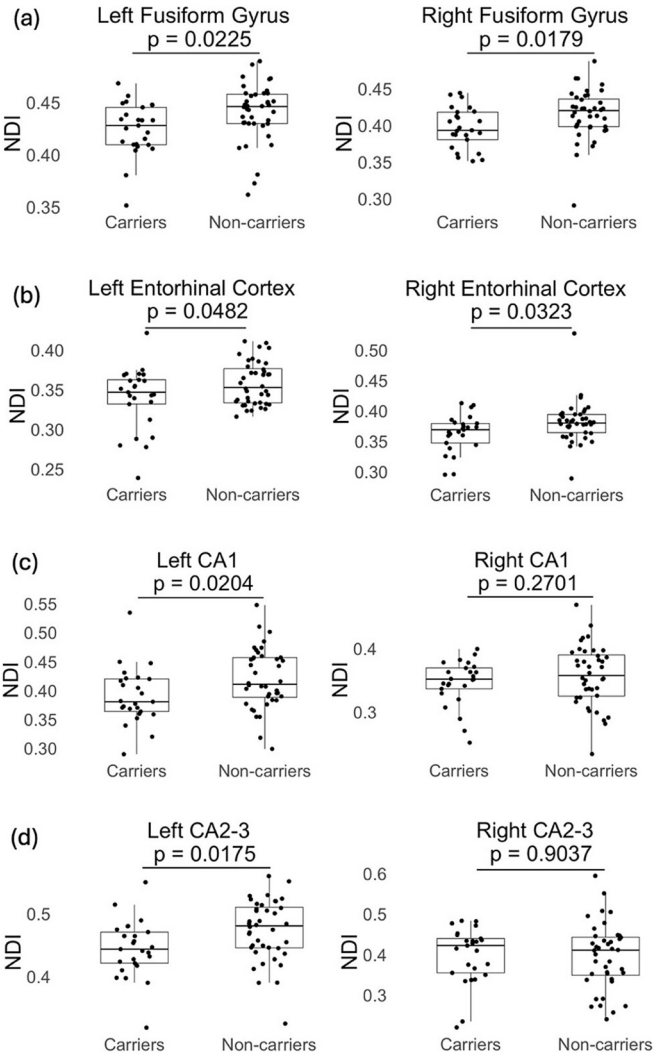

Fig. 1. Neurite density index (NDI) values in the left and right (a) fusiform gyrus, (b) entorhinal cortex, (c) CA1 and (d) CA2-3 regions amongst APOE-e4 carriers and non-carriers.

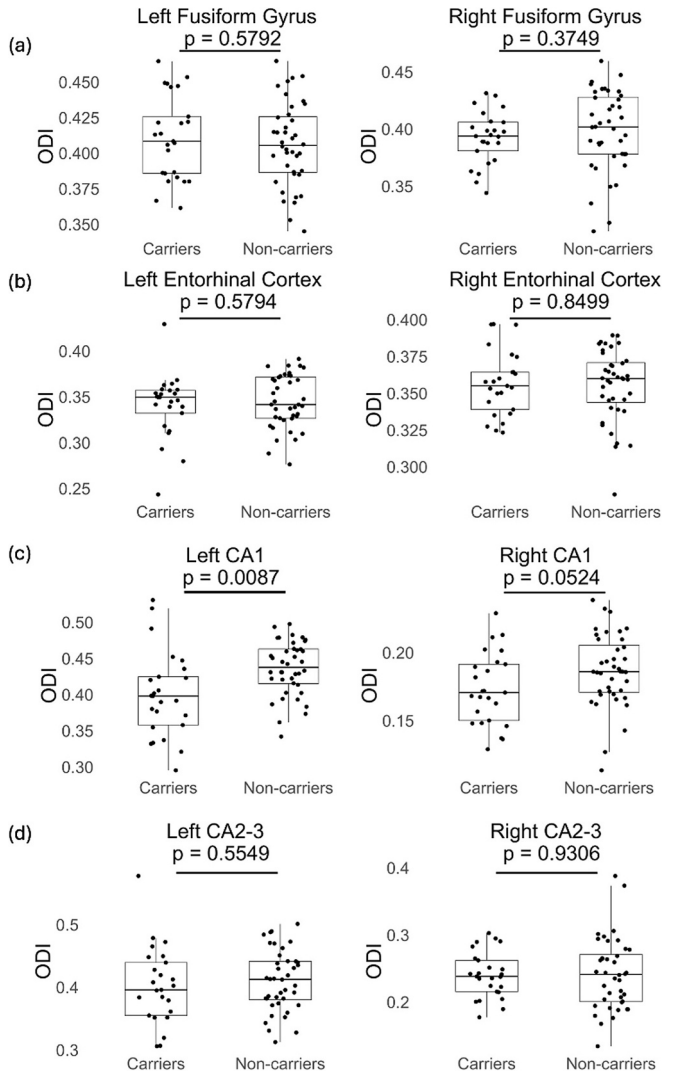

Fig. 2. Orientation dispersion index (ODI) values in the left and right (a) fusiform gyrus, (b) entorhinal cortex, (c) CA1 and (d) CA2-3 regions amongst APOE-e4 carriers and non-carriers.

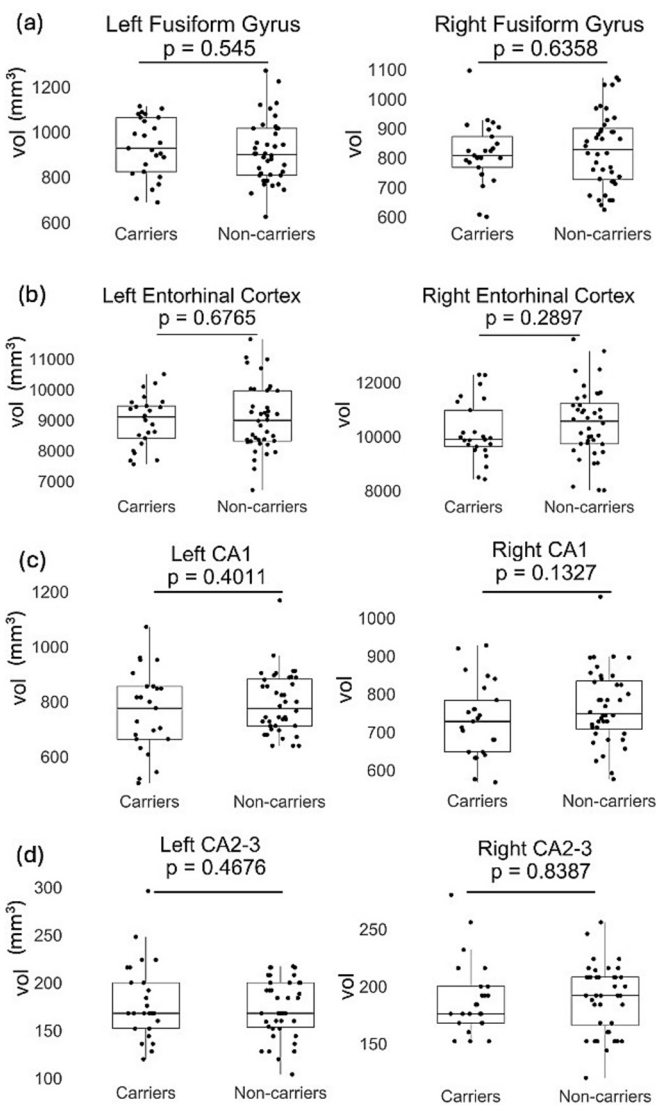

Fig. 3. Volumetric analysis values (vol) in the left and right (a) fusiform gyrus, (b) entorhinal cortex, (c) CA1 and (d) CA2-3 regions amongst APOE-e4 carriers and non-carriers.

significantly different within the left hippocampal subfield regions CA1 (β = 0.03, 95 % CI = [0.005; 0.06], p = 0.02) (Fig. 1c) and CA2–3 (β = 0.03, 95 % CI = [0.005; 0.05], p = 0.02) (Fig. 1d) between carriers and non-carriers, although the right hippocampus subfield regions showed no significant differences in NDI values based on carrier status (right CA1: β = 0.01, 95 % CI = [−0.01; 0.03], p = 0.27; right CA2–3: β = −0.002, 95 % CI = [−0.04; 0.04], p = 0.9).

ODI values for these regions displayed significant differences between carriers and non-carriers only in the left CA1 (β = 0.037, 95 % CI = [0.013; 0.06], p = 0.008) and right CA1 (β = 0.013, 95 % CI = [−0.0001; 0.03], p = 0.052) (Fig. 2c) subfields. All other ROIs were not significantly different between groups: left fusiform gyrus (β = −0.004, 95 % CI = [−0.019; 0.010], p = 0.578), right fusiform gyrus (β = 0.006, 95 % CI = [−0.009; 0.02], p = 0.420) (Fig. 2a), left entorhinal cortex (β = 0.005, 95 % CI = [−0.011; 0.021], p = 0.563); right entorhinal cortex (β = −0.001, 95 % CI = [−0.013; 0.011], p = 0.853) (Fig. 2b); left CA2–3 (β = 0.009, 95 % CI = [−0.018; 0.036], p = 0.532) and, right CA2–3 (β = 0.0009, 95 % CI = [−0.022; 0.025], p = 0.937) (Fig. 2d).

In contrast, no difference in carrier status was observed when analyzed using the standard volumetric measurement for the left fusiform gyrus (β = −21.03, 95 % CI = [−90.99; 48.94], p = 0.54), right fusiform gyrus (β = 13.65, 95 % CI = [−46.29; 73.58], p = 0.64) (Fig. 3a), left entorhinal cortex (β = 99.93, 95 % CI = [−407.85; 607.70], p = 0.68) or right entorhinal cortex (β = 315.85, 95 % CI = [−300.31; 932.01], p = 0.29) (Fig. 3b), left CA1 (β = 29.01, 95 % CI = [−34.94; 92.96], p = 0.40), right CA1 (β = 39.17, 95 % CI = [−11.39; 89.74], p = 0.13) (Fig. 3c), left CA2–3 (β = −6.92, 95 % CI = [−24.51; 10.67], p = 0.47), right CA2–3 (β = 1.60, 95 % CI = [−13.83; 17.03], p = 0.84) (Fig. 3d).

Fig. 4 show that MoCA scores were not significantly different between carriers and non-carriers (β = 0.51, 95 % CI = [−0.88; 1.90], p = 0.51), which was expected given that all participants were asymptomatic. Thus, the groups were collapsed across carrier status to evaluate the extent to which MoCA scores varied as a function of dMRI and standard volumetric measures in the specific regions of interest (Figs. 5 and 6). NDI correlated with MoCA scores in left entorhinal cortex (raw p = 0.05), right entorhinal cortex (raw p = 0.001), left fusiform gyrus (raw p = 0.02) and right CA2–3 (raw p = 0.02) regions. Neither ODI nor standard volumetric measures showed a strong association with MoCA scores. The increased sensitivity of NDI relative to standard volumetric methods to global cognition as well as APOE-e4 carrier status is illustrated in Table 2.

Table 1
Neuroimaging results of left (L) and right (R) ROIs for cognitively unimpaired older adults stratified by carrier status: APOE-e4 carriers (e4+) and non-carriers (e4−).

Metric	ROI	e4− (n = 40)	e4+ (n = 25)	p-Value (FDR)	t-Stat	Cohen-d
NDI	L fusiform gyrus	0.44 ± 0.03	0.42 ± 0.03	0.022*	2.615	0.667
	R fusiform gyrus	0.42 ± 0.03	0.39 ± 0.03	0.018*	3.922	1
	L entorhinal cortex	0.36 ± 0.03	0.33 ± 0.03	0.048*	3.922	1
	R entorhinal cortex	0.38 ± 0.03	0.36 ± 0.03	0.032*	2.615	0.667
	L CA1	0.42 ± 0.03	0.39 ± 0.05	0.020*	2.711	0.772
	R CA1	0.36 ± 0.05	0.35 ± 0.04	0.270	0.889	0.215
	L CA2-3	0.47 ± 0.05	0.44 ± 0.05	0.017*	2.353	0.6
	R CA2-3	0.40 ± 0.08	0.40 ± 0.07	0.903	0	0
ODI	L fusiform gyrus	0.41 ± 0.03	0.41 ± 0.03	0.578	0	0
	R fusiform gyrus	0.40 ± 0.04	0.40 ± 0.02	0.420	0	0
	L entorhinal cortex	0.34 ± 0.03	0.34 ± 0.03	0.563	0	0
	R entorhinal cortex	0.36 ± 0.02	0.36 ± 0.02	0.853	0	0
	L CA1	0.44 ± 0.04	0.40 ± 0.06	0.008*	2.949	0.823
	R CA1	0.19 ± 0.03	0.17 ± 0.03	0.052*	2.615	0.667
	L CA2-3	0.41 ± 0.05	0.40 ± 0.06	0.532	0.696	0.185
	R CA2-3	0.24 ± 0.05	0.24 ± 0.03	0.937	0	0
Volume (vol) (in mm^3)	L fusiform gyrus	912 ± 140	932 ± 130	0.545	−0.586	−0.147
	R fusiform gyrus	828 ± 125	814 ± 103	0.636	0.49	0.12
	L entorhinal cortex	9062 ± 1008	8962 ± 900	0.678	0.416	0.103
	R entorhinal cortex	10,498 ± 1200	10,182 ± 1100	0.299	1.088	0.272
	L CA1	793 ± 110	764 ± 150	0.401	0.836	0.229
	R CA1	766 ± 97	727 ± 102	0.133	1.528	0.394
	L CA2-3	174 ± 30	180 ± 40	0.468	−0.645	−0.176
	R CA2-3	190 ± 29	189 ± 31	0.839	0.13	0.034

L: left; R: right.
* Statistically significant result (false discovery rate corrected (FDR) $p \leq 0.05$).

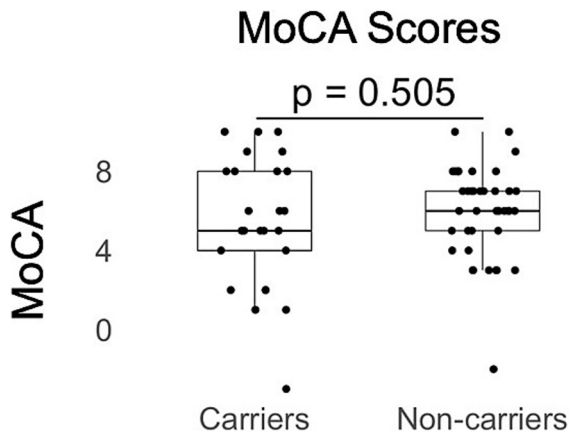

Fig. 4. Montreal Cognitive Assessment (MoCA) test scores amongst APOE-e4 carriers and non-carriers.

4. Discussion

This study used advanced diffusion MRI metric, in this case those derived using the NODDI model, to compare microstructural integrity between cognitively unimpaired APOE-e4 carriers and non-carriers in key brain regions associated with AD pathogenesis. As expected, neurite density (as measured by the NODDI-derived NDI parameter) was lower in the fusiform gyrus, entorhinal cortex and left hippocampal regions of carriers of the APOE-e4 allele when compared against non-carriers, although no such differences were observed in the right hippocampus. Results also showed that NDI values were sensitive to global cognition (measured as MoCA score) and APOE-e4 carrier status. Standard structural MRI-based volumetric measures showed no sensitivity to carrier status and ODI associated with carrier status only in the left and right CA1 regions. Neither volumetric measures nor ODI associated with MoCA performance. These results collectively support the hypothesis that, in individuals at genetic risk for developing AD, NDI is sensitive to early microstructural changes in brain regions that are selectively affected by AD, even before symptom onset.

Our results are reflective of and supported by several studies using the ADNI dataset, which have shown an association between early onset AD and NDI/ODI measures in the entorhinal, middle temporal, inferior temporal, fusiform, precuneus, and precentral areas (Parker et al., 2018; Colgan et al., 2016; Fu et al., 2020; Billiet et al., 2015). Additionally, research outside of the ADNI dataset has validated NDI and ODI values in cortical regions like the fusiform gyrus and entorhinal cortex amongst participants with mild cognitive impairment (MCI) and AD, as well as similar age-related microstructural deficits (Du et al., 2021; Parker et al., 2018; Colgan et al., 2016; Fu et al., 2020; Billiet et al., 2015). Our study significantly expands on these efforts by focusing on NODDI-measured microstructural deficits in people that are *cognitively normal* yet at genetic risk of developing AD (here, carriers of the APOE-e4 allele). Taken collectively, there is strong support of NDI as an early indicator of neurodegeneration. The fact that NDI can detect microstructural changes within brain regions that may eventually show marked pathology supports the use of advanced dMRI and biophysical modelling methods to longitudinally monitoring disease progression, particularly in the prodromal stages of AD.

While ODI was assessed in our study of cognitively normal subjects at genetic risk for AD, it was sensitive to APOE-e4 carrier status in fewer brain regions, and it did not associate with MoCA performance in our study. Since ODI measures the variability in neurite orientations (i.e., how dispersed or aligned the neurites are) it may, in theory, be more relevant as the disease progresses, when extensive disorganization and loss of neurite coherence become more evident due to more pronounced structural changes (Jack and Holtzman, 2013; Weston et al., 2023; Vogt et al., 2020) and, ultimately, measurable differences using standard diffusion tensor imaging and tractography (Zhuang et al., 2013; Jeurissen et al., 2013). Furthermore, increased neurite orientation dispersion (ODI) can reflect different processes depending on context. In healthy individuals, elevated ODI may indicate dendritic complexity or adaptive remodeling (Qiu et al., 2017). However, in neurodegenerative conditions like AD, increased ODI more likely reflects microstructural disorganization and loss of structural coherence (Vogt et al., 2020). Thus, while not inherently pathological, elevated ODI in disease states is typically interpreted as reduced neurite integrity (Sato et al., 2017; Qian et al., 2025; Matsuoka et al., 2020).

In the context of early detection of Alzheimer's disease, diffusion

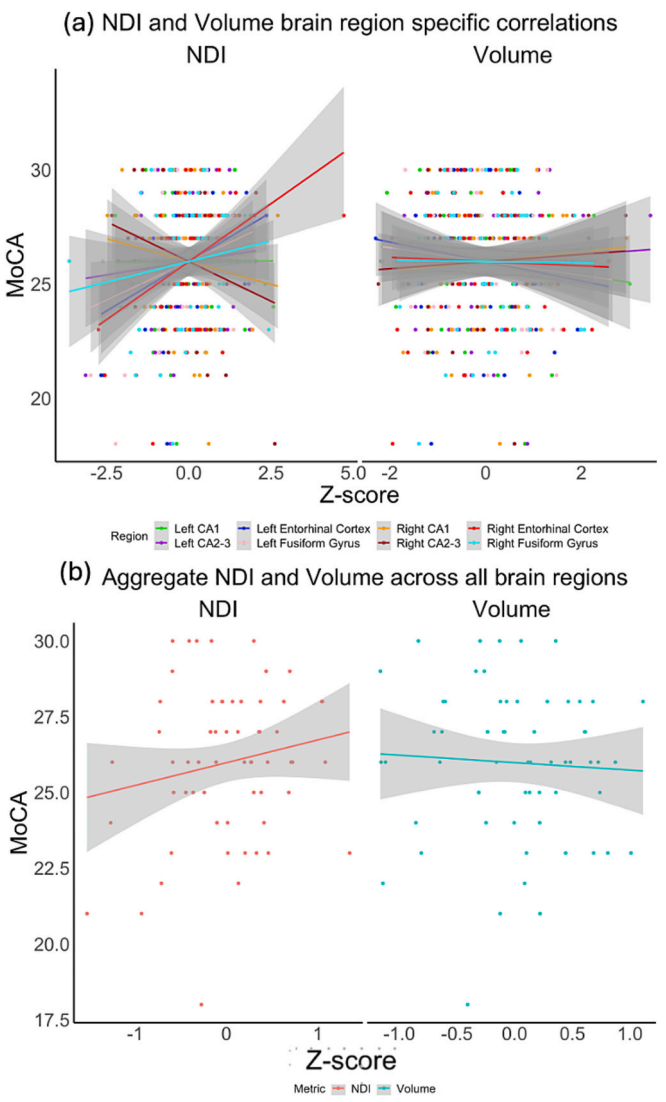

Fig. 5. (a) Plots showing correlation between NDI and MoCA scores in the left and right CA1, CA2-3, entorhinal cortex and fusiform gyrus. (b) Aggregate NDI and volume measures for each participant across all brain regions regressed to MoCA score.

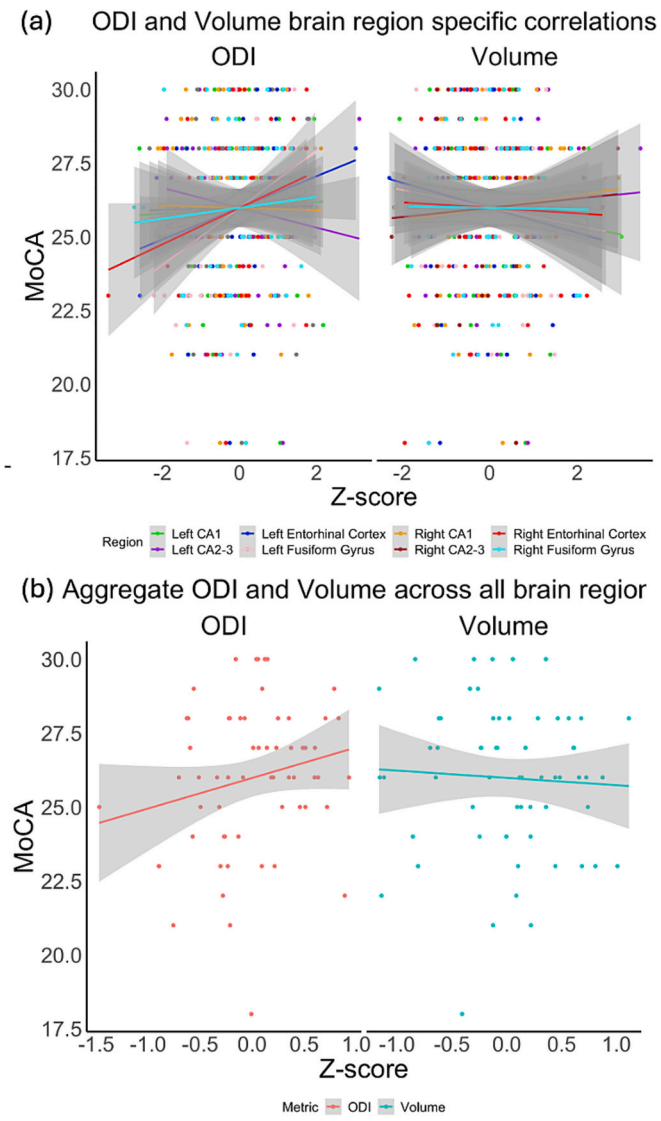

Fig. 6. (a) Plots showing correlation between ODI and MoCA scores the left and right CA1, CA2–3, entorhinal cortex and fusiform gyrus. (b) Aggregate ODI and volume measures for each participant across all brain regions regressed to MoCA score.

tensor imaging (DTI) metrics such as fractional anisotropy (FA) and mean diffusivity (MD) are widely used but are limited by their inability to differentiate the specific biophysical contributors of the diffusion signals. In contrast, NODDI models the diffusion-weighted signal using a three-compartment framework—capturing intra-neurite (restricted), extra-neurite (hindered), and isotropic (free water) diffusion components—allowing for more biologically specific metrics such as neurite density index (NDI) and orientation dispersion index (ODI). Prior studies (Kamiya et al., 2020; Colgan et al., 2016) have demonstrated that NODDI offers superior sensitivity to early microstructural degeneration in neurodegenerative disorders, such as AD. This helps particularly in regions where DTI metrics are confounded by problems such as crossing fibers or partial volume effects. Our findings align with this notion, as NDI values were significantly lower in APOE-e4 carriers and correlated with global cognition, illustrating its sensitivity to early neurite degeneration and its relevance for detecting preclinical AD-related microstructural changes.

Results from this study are also consistent with prior work showing less connectivity of the left hippocampus with the rest of brain relative to the right hippocampus in cognitively unimpaired older adults who are APOE-e4 carriers (Caselli et al., 2004; Baxter et al., 2023), and that the extent of left (but not right) hippocampal connectivity was correlated with verbal memory scores (Baxter et al., 2023). Other studies (Abraham et al., 2020; Jessen et al., 2006; Mohtasib et al., 2022) further support that AD progression affects the hippocampus asymmetrically, highlighting the critical role of left hemisphere microstructural differences linked to the APOE-e4 allele in early cognitive decline in at-risk individuals. This likely explains, in part, the differences in NDI values between APOE e4 carriers and non-carriers within the left but not right hippocampal subfields. This study does not, however, address whether microstructural changes within the left hippocampus precede or are concurrent with connectivity and cognitive changes, which can be explored in the future with longitudinal cohorts and rodent imaging studies.

A key limitation of this study lies in the degree to which the NODDI biophysical model accurately reflects non-white matter tissue microstructure. NODDI was originally "tuned" for assessment of white matter structures (Parker et al., 2018; Billiet et al., 2015; Pines et al., 2020) and thus makes key model assumptions about the tissue that do not completely reflect the "mixed" nature of subcortical structures like the hippocampus (i.e., cell bodies, unmyelinated axons, and myelinated

Table 2
Individual relationship for each brain region based on either volume or NODDI metric quantification to MoCA. Statistical results are reported here along with the estimated slope between each measure and MoCA. Adjusted p-value was calculated using a false discovery rate correction (FDR).

ROI/metric	Slope estimate	Adjusted p-value (FDR)	r
Left entorhinal cortex/NDI	0.6620	0.2044	0.344
Right entorhinal cortex/NDI	0.9583	0.0217*	0.268
Left fusiform gyrus/NDI	0.8059	0.0943	0.404
Right fusiform gyrus/NDI	0.3362	0.6422	0.144
Left CA1/NDI	−0.0279	0.9298	0.004
Right CA1/NDI	−0.5208	0.3324	0.093
Left CA2-3/NDI	0.2365	0.6422	−0.16
Right CA2-3/NDI	−0.7308	0.0943	−0.277
Left entorhinal cortex/ODI	0.2158	0.8945	0.213
Right entorhinal cortex/ODI	0.4633	0.8989	0.246
Left fusiform gyrus/ODI	0.7522	0.4052	0.386
Right fusiform gyrus/ODI	−0.0707	0.9029	0.074
Left CA1/ODI	−0.0462	0.9029	0.038
Right CA1/ODI	−0.1466	0.9029	−0.016
Left CA2-3/ODI	−0.3112	0.9134	−0.134
Right CA2-3/ODI	0.0344	0.9134	0.065
Left entorhinal cortex/ volume	0.6150	0.7096	−0.169
Right entorhinal cortex/ volume	0.4709	0.6422	−0.12
Left fusiform gyrus/volume	0.4384	0.6422	−0.037
Right fusiform gyrus/volume	0.4522	0.6422	−0.011
Left CA1/volume	0.2299	0.5749	−0.12
Right CA1/volume	0.8462	0.9067	0.061
Left CA2-3/volume	0.6046	0.7096	0.086
Right CA2-3/volume	0.0385	0.9029	0.063

* Statistically significant result (false discovery rate corrected (FDR) $p \leq 0.05$).

axons all existing within a single voxel), nor does it account for potential exchange of water across cellular compartments. Nevertheless, given the acquisition scheme of the dataset used, our focus on neurite microstructure, and the uncertain importance of exchange in biophysical models of diffusion in the brain given real-world clinical datasets (Jelescu et al., 2022; Yang et al., 2018; Schiavi et al., 2023), NODDI was deemed the most robust biophysical model for this preliminary study of subcortical microstructure in asymptomatic APOE e4 carrier and non-carrier groups. Still, the inability of NODDI to quantify microstructural detail about the soma (gray matter) or cellular exchange across tissue microenvironments, both of which may be critical to AD progression and treatment (Jelescu et al., 2020; Nazeri et al., 2020; Gatto, 2020; Figini, 2014; Singh et al., 2024), is an important limitation of this work. Future work will focus on optimization of data acquisition parameters for more complex diffusion models such as soma and neurite density imaging (SANDI) (Palombo et al., 2020) and/or neurite exchange imaging (NEXI) (Jelescu et al., 2022), which will capture and/or mitigate these potentially important parameters. Finally, the relatively small sample size, particularly of carriers, and the cross-sectional nature of this study limits the generalizability of the findings. Future studies with larger cohorts are needed to confirm these results and enhance the statistical power of the analyses. Despite this limitation, the observed trends provide valuable insights into the potential impact of APOE-e4 status on very early microstructural changes to the brain that might be pathologically relevant to the progression of AD.

This study used NODDI analyses of diffusion MRI to show microstructural differences between cognitively intact APOE-e4 carriers and non-carriers, specifically in the fusiform gyrus, entorhinal cortex and left hippocampal subfields (CA1, CA2-3). These results are particularly promising, given that more conventional MRI methods (i.e., T1-weighted imaging) and cognitive screening tools (i.e., MoCA) were not sensitive to differences between these groups who have differential genetic risk for AD. This study therefore suggests that dMRI could be used to: (i) study AD progression at very early, asymptomatic stages, (ii) potentially stratify AD risk within asymptomatic individuals at early stages, and (iii) monitor disease progression over time, particularly in the prodromal stages of AD.

CRediT authorship contribution statement

Sasha Hakhu: Writing – original draft, Visualization, Validation, Software, Methodology, Investigation, Data curation, Conceptualization. **Andrew Hooyman:** Writing – review & editing, Visualization, Supervision, Software, Formal analysis. **Jennapher Lingo VanGilder:** Writing – review & editing, Supervision, Methodology. **Sydney Y. Schaefer:** Writing – review & editing, Validation, Supervision, Investigation. **Scott C. Beeman:** Writing – review & editing, Supervision, Investigation, Conceptualization.

Consent statement

All human subjects participating in studies conducted by the Alzheimer's Disease Neuroimaging Initiative (ADNI), provided informed consent.

Funding sources

No funding to disclose at this moment.

Declaration of competing interest

There are no conflicts of interest to declare.

Acknowledgments

Data collection and sharing for this project was funded by the Alzheimer's Disease Neuroimaging Initiative (ADNI) (National Institutes of Health Grant U01 AG024904) and DOD ADNI (Department of Defense award number W81XWH-12-2-0012). ADNI is funded by the National Institute on Aging, the National Institute of Biomedical Imaging and Bioengineering, and through generous contributions from the following: AbbVie, Alzheimer's Association; Alzheimer's Drug Discovery Foundation; Araclon Biotech; BioClinica, Inc.; Biogen; Bristol-Myers Squibb Company; CereSpir, Inc.; Cogstate; Eisai Inc.; Elan Pharmaceuticals, Inc.; Eli Lilly and Company; EuroImmun; F. Hoffmann-La Roche Ltd. and its affiliated company Genentech, Inc.; Fujirebio; GE Healthcare; IXICO Ltd.;Janssen Alzheimer Immunotherapy Research & Development, LLC.; Johnson & Johnson Pharmaceutical Research & Development LLC.; Lumosity; Lundbeck; Merck & Co., Inc.; Meso Scale Diagnostics, LLC.; NeuroRx Research; Neurotrack Technologies; Novartis Pharmaceuticals Corporation; Pfizer Inc.; Piramal Imaging; Servier; Takeda Pharmaceutical Company; and Transition Therapeutics. The Canadian Institutes of Health Research is providing funds to support ADNI clinical sites in Canada. Private sector contributions are facilitated by the Foundation for the National Institutes of Health (www.fnih.org). The grantee organization is the Northern California Institute for Research and Education, and the study is coordinated by the Alzheimer's Therapeutic Research Institute at the University of Southern California. ADNI data are disseminated by the Laboratory for Neuro Imaging at the University of Southern California.

Dr. Scott Beeman and Dr. Sydney Schaefer are affiliated with the Arizona Alzheimer's Consortium, and Dr. Schaefer is a REC Fellow of the Arizona Alzheimer's Disease Research Center (P30 AG072980).

References

Abraham, M., Seidenberg, M., Kelly, D.A., et al., 2020. Episodic memory and hippocampal volume predict five-year MCI conversion in healthy APOE ε4 carriers. J. Int. Neuropsychol. Soc. JINS. 26 (7), 733–738. https://doi.org/10.1017/S1355617720000181.

ADNI. Alzheimer'sDisease NeuroImaging III (ADNI3) Study 3T. https://adni.loni.usc.edu/wp-content/themes/freshnews-dev-v2/documents/mri/ADNI3_MRI_Tech_Manual_v2.pdf.
ADNI. Alzheimer's Disease Neuro Imaging III (ADNI3) MRI analysis user document MRI analysis processing pipeline suggestions and tips. https://adni.loni.usc.edu/wp-content/themes/freshnews-dev-v2/documents/mri/ADNI3_MRI_Analysis_Manual_20180202.pdf.
Albert, M.S., Moss, M.B., Tanzi, R., Jones, K., 2001. Preclinical prediction of AD using neuropsychological tests. J. Int. Neuropsychol. Soc. 7 (5), 631–639. https://doi.org/10.1017/S1355617701755105.
Albert, S.M., Glied, S., Andrews, H., Stern, Y., Mayeux, R., 2002. Primary care expenditures before the onset of Alzheimer's disease. Neurology 59 (4), 573–578. https://doi.org/10.1212/WNL.59.4.573.
Amunts, K., Kedo, O., Kindler, M., et al., 2005. Cytoarchitectonic mapping of the human amygdala, hippocampal region and entorhinal cortex: intersubject variability and probability maps. Anat Embryol (Berl). 210 (5–6), 343–352. https://doi.org/10.1007/s00429-005-0025-5.
Andersson, J.L.R.. Non-linear registration aka spatial normalisation. https://www.fmrib.ox.ac.uk/datasets/techrep/tr07ja2/tr07ja2.pdf. (Accessed 7 March 2024).
Andersson, J.L.R., Sotiropoulos, S.N., 2016. An integrated approach to correction for off-resonance effects and subject movement in diffusion MR imaging. NeuroImage 125, 1063–1078. https://doi.org/10.1016/j.neuroimage.2015.10.019.
Baxter, L.C., Limback-Stokin, M., Patten, K.J., et al., 2023. Hippocampal connectivity and memory decline in cognitively intact APOE ε4 carriers. Alzheimers Dement. 19 (9), 3806–3814. https://doi.org/10.1002/alz.13023.
Berghuis, K.M.M., Fagioli, S., Maurits, N.M., et al., 2019. Age-related changes in brain deactivation but not in activation after motor learning. NeuroImage 186, 358–368. https://doi.org/10.1016/j.neuroimage.2018.11.010.
Billiet, T., Vandenbulcke, M., Mädler, B., et al., 2015. Age-related microstructural differences quantified using myelin water imaging and advanced diffusion MRI. Neurobiol. Aging 36 (6), 2107–2121. https://doi.org/10.1016/j.neurobiolaging.2015.02.029.
Bo, J., Seidler, R.D., 2009. Visuospatial working memory capacity predicts the organization of acquired explicit motor sequences. J. Neurophysiol. 101 (6), 3116–3125. https://doi.org/10.1152/jn.00006.2009.
Burggren, A., Brown, J., 2014. Imaging markers of structural and functional brain changes that precede cognitive symptoms in risk for Alzheimer's disease. Brain Imaging Behav. 8 (2), 251–261. https://doi.org/10.1007/s11682-013-9278-4.
Caselli, R.J., Reiman, E.M., Osborne, D., et al., 2004. Longitudinal changes in cognition and behavior in asymptomatic carriers of the APOE e4 allele. Neurology 62 (11), 1990–1995. https://doi.org/10.1212/01.WNL.0000129533.26544.BF.
Colgan, N., Siow, B., O'Callaghan, J.M., et al., 2016. Application of neurite orientation dispersion and density imaging (NODDI) to a tau pathology model of Alzheimer's disease. NeuroImage 125, 739–744. https://doi.org/10.1016/j.neuroimage.2015.10.043.
Desikan, R.S., Ségonne, F., Fischl, B., et al., 2006. An automated labeling system for subdividing the human cerebral cortex on MRI scans into gyral based regions of interest. NeuroImage 31 (3), 968–980. https://doi.org/10.1016/j.neuroimage.2006.01.021.
Devanand, D.P., Bansal, R., Liu, J., Hao, X., Pradhaban, G., Peterson, B.S., 2012. MRI hippocampal and entorhinal cortex mapping in predicting conversion to Alzheimer's disease. NeuroImage 60 (3), 1622–1629. https://doi.org/10.1016/j.neuroimage.2012.01.075.
Douaud, G., Menke, R.A.L., Gass, A., et al., 2013. Brain microstructure reveals early abnormalities more than two years prior to clinical progression from mild cognitive impairment to Alzheimer's disease. J. Neurosci. 33 (5), 2147–2155. https://doi.org/10.1523/JNEUROSCI.4437-12.2013.
Du, J., Liu, Z., Hanford, L.C., et al., 2021. Exploration of Alzheimer's Disease MRI Biomarkers Using APOE4 Carrier Status in the UK Biobank. https://doi.org/10.1101/2021.09.09.21263324 (2021.09.09.21263324, Published online September 14).
Evans, S.L., Dowell, N.G., Prowse, F., Tabet, N., King, S.L., Rusted, J.M., 2020. Mid age APOE ε4 carriers show memory-related functional differences and disrupted structure-function relationships in hippocampal regions. Sci. Rep. 10 (1), 3110. https://doi.org/10.1038/s41598-020-59272-0.
Figini, M., 2014. Model-based analysis of diffusion magnetic resonance: study of microstructural damage in white matter and gray matter diseases. https://www.politesi.polimi.it/handle/10589/97955. (Accessed 5 August 2024) (Published online September 30).
Frisoni, G.B., Fox, N.C., Jack, C.R., Scheltens, P., Thompson, P.M., 2010. The clinical use of structural MRI in Alzheimer disease. Nat. Rev. Neurol. 6 (2), 67–77. https://doi.org/10.1038/nrneurol.2009.215.
Fu, X., Shrestha, S., Sun, M., et al., 2020. Microstructural white matter alterations in mild cognitive impairment and Alzheimer's disease. Clin. Neuroradiol. 30 (3), 569–579. https://doi.org/10.1007/s00062-019-00805-0.
Gatto, R.G., 2020. Molecular and microstructural biomarkers of neuroplasticity in neurodegenerative disorders through preclinical and diffusion magnetic resonance imaging studies. J. Integr. Neurosci. 19 (3), 571–592. https://doi.org/10.31083/j.jin.2020.03.165.
Gordon, B.A., Zacks, J.M., Blazey, T., et al., 2015. Task-evoked fMRI changes in attention networks are associated with preclinical Alzheimer's disease biomarkers. Neurobiol. Aging 36 (5), 1771–1779. https://doi.org/10.1016/j.neurobiolaging.2015.01.019.
Goveas, J., O'Dwyer, L., Mascalchi, M., Cosottini, M., Diciotti, S., De Santis, S., Passamonti, L., Tessa, C., Toschi, N., Giannelli, M., 2015. Diffusion-MRI in neurodegenerative disorders. Magn. Reson. Imaging 33 (7), 853–876. https://doi.org/10.1016/j.mri.2015.04.006.
Hamza, Eid A., Moustafa, Ahmed A., Tindle, Richard, et al., 2022. Effect of APOE4 allele and gender on the rate of atrophy in the hippocampus, entorhinal cortex, and fusiform gyrus in Alzheimer's disease. Curr. Alzheimer Res. 19, 943–953. https://doi.org/10.2174/1567205020666230309113749.
Hoy, A.R., Ly, M., Carlsson, C.M., et al., 2017. Microstructural white matter alterations in preclinical Alzheimer's disease detected using free water elimination diffusion tensor imaging. PLoS One 12 (3), e0173982. https://doi.org/10.1371/journal.pone.0173982.
Montal, V., Vilaplana, E., Alcolea, D., Pegueroles, J., Pasternak, O., González-Ortiz, S., Fortea, J., 2018. Cortical microstructural changes along the Alzheimer's disease continuum. Alzheimer's & Dementia 14 (3), 340–351. https://doi.org/10.21203/rs.3.rs-3921380/v1.
https://www.bic.mni.mcgill.ca/ServicesAtlases/HomePage. (Accessed 7 March 2024).
R: The R Project for Statistical Computing. https://www.r-project.org/. (Accessed 25 January 2024).
Jack, C.R., Holtzman, D.M., 2013. Biomarker modeling of Alzheimer's disease. Neuron 80 (6), 1347–1358. https://doi.org/10.1016/j.neuron.2013.12.003.
Jelescu, I.O., Palombo, M., Bagnato, F., Schilling, K.G., 2020. Challenges for biophysical modeling of microstructure. J. Neurosci. Methods 344, 108861. https://doi.org/10.1016/j.jneumeth.2020.108861.
Jelescu, I.O., de Skowronski, A., Geffroy, F., Palombo, M., Novikov, D.S., 2022. Neurite Exchange Imaging (NEXI): a minimal model of diffusion in gray matter with inter-compartment water exchange. NeuroImage 256, 119277. https://doi.org/10.1016/J.NEUROIMAGE.2022.119277.
Jenkinson, M., Bannister, P., Brady, M., Smith, S., 2002. Improved optimization for the robust and accurate linear registration and motion correction of brain images. NeuroImage 17 (2), 825–841. https://doi.org/10.1016/s1053-8119(02)91132-8.
Jenkinson, M., Beckmann, C.F., Behrens, T.E.J., Woolrich, M.W., Smith, S.M., 2012. FSL. NeuroImage 62 (2), 782–790. https://doi.org/10.1016/j.neuroimage.2011.09.015.
Jessen, F., Feyen, L., Freymann, K., et al., 2006. Volume reduction of the entorhinal cortex in subjective memory impairment. Neurobiol. Aging 27 (12), 1751–1756. https://doi.org/10.1016/j.neurobiolaging.2005.10.010.
Jeurissen, B., Leemans, A., Tournier, J.D., Jones, D.K., Sijbers, J., 2013. Investigating the prevalence of complex fiber configurations in white matter tissue with diffusion magnetic resonance imaging. Hum. Brain Mapp. 34 (11), 2747–2766. https://doi.org/10.1002/hbm.22099.
Kamiya, K., Hori, M., Aoki, S., 2020. NODDI in clinical research. J. Neurosci. Methods 346, 108908. https://doi.org/10.1016/j.jneumeth.2020.108908.
Killiany, R.J., Hyman, B.T., Gomez-Isla, T., et al., 2002. MRI measures of entorhinal cortex vs hippocampus in preclinical AD. Neurology 58 (8), 1188–1196. https://doi.org/10.1212/WNL.58.8.1188.
Landau, S.M., Harvey, D., Madison, C.M., et al., 2011. Associations between cognitive, functional, and FDG-PET measures of decline in AD and MCI. Neurobiol. Aging 32 (7), 1207–1218. https://doi.org/10.1016/j.neurobiolaging.2009.07.002.
Langan, J., Seidler, R.D., 2011. Age differences in spatial working memory contributions to visuomotor adaptation and transfer. Behav. Brain Res. 225 (1), 160–168. https://doi.org/10.1016/j.bbr.2011.07.014.
Locke, P.A., Conneally, P.M., Tanzi, R.E., Gusella, J.F., Haines, J.L., 1995. Apolipoprotein E4 allele and Alzheimer disease: examination of allelic association and effect on age at onset in both early-and late-onset cases. Genet. Epidemiol. 12 (1), 83–92. https://doi.org/10.1002/gepi.1370120108.
Ma, D., Fetahu, I.S., Wang, M., et al., 2020. The fusiform gyrus exhibits an epigenetic signature for Alzheimer's disease. Clin. Epigenetics 12 (1), 129. https://doi.org/10.1186/s13148-020-00916-3.
Mak, E., Reid, R.I., Przybelski, S.A., Lesnick, T.G., Schwarz, C.G., Senjem, M.L., Kantarci, K., 2023. Alzheimer's disease biomarkers of amyloid and tau influence white matter neurite alterations in dementia with Lewy bodies: a NODDI study. Alzheimer's & Dementia 19, e076922. https://doi.org/10.1002/alz.076922.
Mak, E., Dounavi, M.E., Operto, G., Ziukelis, E.T., Jones, P.S., Low, A., O'Brien, J.T., 2024. APOE ε4 exacerbates age-dependent deficits in cortical microstructure. Brain Communications 6 (1), fcad351. https://doi.org/10.1093/braincomms/fcad351.
Malek-Ahmadi, M., Duff, K., Chen, K., et al., 2023. Volumetric regional MRI and neuropsychological predictors of motor task variability in cognitively unimpaired, Mild Cognitive Impairment, and probable Alzheimer's disease older adults. Exp. Gerontol. 173, 112087. https://doi.org/10.1016/J.EXGER.2023.112087.
Matsuoka, K., Makinodan, M., Kitamura, S., et al., 2020. Increased dendritic orientation dispersion in the left occipital gyrus is associated with atypical visual processing in adults with autism spectrum disorder. Cereb. Cortex 30 (11), 5617–5625. https://doi.org/10.1093/cercor/bhaa121.
Microstructure Imaging Group. Download NODDI matlab toolbox. http://mig.cs.ucl.ac.uk/index.php?n=Download.NODDI. (Accessed 25 January 2024).
Mohtasib, R., Alghamdi, J., Jobeir, A., et al., 2022. MRI biomarkers for Alzheimer's disease: the impact of functional connectivity in the default mode network and structural connectivity between lobes on diagnostic accuracy. Heliyon 8 (2), e08901. https://doi.org/10.1016/j.heliyon.2022.e08901.
Mukherji, D., Mukherji, M., Mukherji, N., Alzheimer's disease neuroimaging initiative, 2022. Early detection of Alzheimer's disease using neuropsychological tests: a predict–diagnose approach using neural networks. Brain Inform. 9 (1), 23. https://doi.org/10.1186/s40708-022-00169-1.
Nazeri, A., Schifani, C., Anderson, J.A.E., Ameis, S.H., Voineskos, A.N., 2020. In vivo imaging of gray matter microstructure in major psychiatric disorders: opportunities for clinical translation. Biol Psychiatry Cogn Neurosci Neuroimaging. 5 (9), 855–864. https://doi.org/10.1016/j.bpsc.2020.03.003.
Nordberg, A., Rinne, J., Kadir, A., Langstrom, B., 2010. The use of PET in Alzheimer disease. Nat. Rev. Neurol. 6, 78–87. https://doi.org/10.1038/nrneurol.2009.217.

Palombo, M., Ianus, A., Guerreri, M., et al., 2020. SANDI: a compartment-based model for non-invasive apparent soma and neurite imaging by diffusion MRI. NeuroImage 215, 116835. https://doi.org/10.1016/J.NEUROIMAGE.2020.116835.
Parker, T.D., Slattery, C.F., Zhang, J., et al., 2018. Cortical microstructure in young onset Alzheimer's disease using neurite orientation dispersion and density imaging. Hum. Brain Mapp. 39 (7), 3005–3017. https://doi.org/10.1002/hbm.24056.
Pennanen, C., Kivipelto, M., Tuomainen, S., et al., 2004. Hippocampus and entorhinal cortex in mild cognitive impairment and early AD. Neurobiol. Aging 25 (3), 303–310. https://doi.org/10.1016/S0197-4580(03)00084-8.
Pines, A.R., Cieslak, M., Larsen, B., et al., 2020. Leveraging multi-shell diffusion for studies of brain development in youth and young adulthood. Dev. Cogn. Neurosci. 43, 100788. https://doi.org/10.1016/j.dcn.2020.100788.
Qian, W., Xu, X., Wu, Y., et al., 2025. Altered white matter microstructural integrity in patients with postherpetic neuralgia: a combined DTI and DTI-NODDI study. Front. Neurosci. 19, 1552961. https://doi.org/10.3389/fnins.2025.1552961.
Qiu, A., Alexander, A.L., Edwards, L.J., Pine, Kerrin J., Ellerbrock, Isabel, Weiskopf, Nikolaus, Mohammadi, Siawoosh, 2017. NODDI-DTI: estimating neurite orientation and dispersion parameters from a diffusion tensor in healthy white matter. Front. Neurosci. 11, 720. https://doi.org/10.3389/fnins.2017.00720.
Rao, Y.L., Ganaraja, B., Murlimanju, B.V., Joy, T., Krishnamurthy, A., Agrawal, A., 2022. Hippocampus and its involvement in Alzheimer's disease: a review. 3 Biotech 12 (2), 55. https://doi.org/10.1007/s13205-022-03123-4.
Reiman, E.M., Caselli, R.J., Chen, K., Alexander, G.E., Bandy, D., Frost, J., 2001. Declining brain activity in cognitively normal apolipoprotein E ε4 heterozygotes: a foundation for using positron emission tomography to efficiently test treatments to prevent Alzheimer's disease. Proc. Natl. Acad. Sci. 98 (6), 3334–3339. https://doi.org/10.1073/pnas.061509598.
Saint-Aubert, L., Lemoine, L., Chiotis, K., Leuzy, A., Rodriguez-Vieitez, E., Nordberg, A., 2017. Tau PET imaging: present and future directions. Mol. Neurodegener. 12 (1), 19. https://doi.org/10.1186/s13024-017-0162-3.
Sato, K., Kerever, A., Kamagata, K., Tsuruta, K., Irie, R., Tagawa, K., Aoki, S., 2017. Understanding microstructure of the brain by comparison of neurite orientation dispersion and density imaging (NODDI) with transparent mouse brain. Acta Radiol. Open 6 (4), 2058460117703816. https://doi.org/10.1177/2058460117703816.
Schiavi, S., Palombo, M., Zacà, D., et al., 2023. Mapping tissue microstructure across the human brain on a clinical scanner with soma and neurite density image metrics. Hum. Brain Mapp. 44 (13), 4792–4811. https://doi.org/10.1002/hbm.26416.
Schilling, K.G., Blaber, J., Huo, Y., et al., 2019. Synthesized b0 for diffusion distortion correction (Synb0-DisCo). Magn. Reson. Imaging 64, 62–70. https://doi.org/10.1016/J.MRI.2019.05.008.
Singh, K., Barsoum, S., Schilling, K.G., An, Y., Ferrucci, L., Benjamini, D., 2024. Neuronal microstructural changes in the human brain are associated with neurocognitive aging. Aging Cell 23 (7), e14166. https://doi.org/10.1111/acel.14166.
Slattery, C.F., Zhang, J., Paterson, R.W., et al., 2017. ApoE influences regional white-matter axonal density loss in Alzheimer's disease. Neurobiol. Aging 57, 8–17. https://doi.org/10.1016/j.neurobiolaging.2017.04.021.
Tournier, J.D., 2019. Diffusion MRI in the brain – theory and concepts. Prog. Nucl. Magn. Reson. Spectrosc. 112-113, 1–16. https://doi.org/10.1016/j.pnmrs.2019.03.001.
Tournier, J.D., Smith, R., Raffelt, D., et al., 2019. MRtrix3: a fast, flexible and open software framework for medical image processing and visualisation. NeuroImage 202, 116137. https://doi.org/10.1016/j.neuroimage.2019.116137.
Twamley, E.W., Ropacki, SaL, Bondi, M.W., 2006. Neuropsychological and neuroimaging changes in preclinical Alzheimer's disease. J. Int. Neuropsychol. Soc. 12 (5), 707–735. https://doi.org/10.1017/S1355617706060863.
van Duijn, C.M., de Knijff, P., Cruts, M., et al., 1994. Apolipoprotein E4 allele in a population–based study of early–onset Alzheimer's disease. Nat. Genet. 7 (1), 74–78. https://doi.org/10.1038/ng0594-74.
Vogt, N.M., Hunt, J.F., Adluru, N., et al., 2020. Cortical microstructural alterations in mild cognitive impairment and Alzheimer's disease dementia. Cereb. Cortex 30 (5), 2948–2960. https://doi.org/10.1093/cercor/bhz286.
Weiner, M.W., Veitch, D.P., Aisen, P.S., Beckett, L.A., Cairns, N.J., Green, R.C., Harvey, D., Jack, C.R., Jagust, W., Morris, J.C., Petersen, R.C., Salazar, J., Saykin, A. J., Shaw, L.M., Toga, A.W., Trojanowski, J.Q., Alzheimer's Disease Neuroimaging Initiative, 2017. The Alzheimer's Disease Neuroimaging Initiative 3: continued innovation for clinical trial improvement. Alzheimers Dement. J. Alzheimers Assoc. 13 (5), 561–571. https://doi.org/10.1016/j.jalz.2016.10.006.
Wen, Q., Kelley, D.A.C., Banerjee, S., et al., 2015. Clinically feasible NODDI characterization of glioma using multiband EPI at 7 T. NeuroImage Clin. 9, 291–299. https://doi.org/10.1016/j.nicl.2015.08.017.
Weston, P.S.J., Coath, W., Harris, M.J., et al., 2023. Cortical tau is associated with microstructural imaging biomarkers of neurite density and dendritic complexity in Alzheimer's disease. Alzheimers Dement. 19 (6), 2750–2754. https://doi.org/10.1002/alz.13011.
Xu, Y., Jack, C.R., O'Brien, P.C., Kokmen, E., Smith, G.E., Ivnik, R.J., Boeve, B.F., Tangalos, R.G., Petersen, R.C., 2000. Usefulness of MRI measures of entorhinal cortex versus hippocampus in AD. Neurology 54 (9), 1760–1767. https://doi.org/10.1212/WNL.54.9.1760.
Yang, D.M., Huettner, J.E., Bretthorst, G.L., Neil, J.J., Garbow, J.R., Ackerman, J.J.H., 2018. Intracellular water preexchange lifetime in neurons and astrocytes. Magn. Reson. Med. 79 (3), 1616–1627. https://doi.org/10.1002/mrm.26781.
Yetkin, F.Z., Rosenberg, R.N., Weiner, M.F., Purdy, P.D., Cullum, C.M., 2006. FMRI of working memory in patients with mild cognitive impairment and probable Alzheimer's disease. Eur. Radiol. 16 (1), 193–206. https://doi.org/10.1007/s00330-005-2794-x.
Yu, X., Przybelski, S.A., Reid, R.I., Lesnick, T.G., Raghavan, S., Graff-Radford, J., Lowe, V.J., Kantarci, K., Knopman, D.S., Petersen, R.C., Jack, C.R., Vemuri, P., 2024. NODDI in gray matter is a sensitive marker of aging and early AD changes. Alzheimers Dement. Diagn. Assess. Dis. Monit. 16 (3), e12627. https://doi.org/10.1002/dad2.12627.
Zhang, H., Schneider, T., Wheeler-Kingshott, C.A., Alexander, D.C., 2012. NODDI: practical in vivo neurite orientation dispersion and density imaging of the human brain. NeuroImage 61 (4), 1000–1016. https://doi.org/10.1016/j.neuroimage.2012.03.072.
Zhang, Y., Chen, H., Li, R., Sterling, K., Song, W., 2023. Amyloid β-based therapy for Alzheimer's disease: challenges, successes and future. Signal Transduct. Target. Ther. 8 (1), 1–26. https://doi.org/10.1038/s41392-023-01484-7.
Zhuang, L., Sachdev, P.S., Trollor, J.N., et al., 2013. Microstructural white matter changes, not hippocampal atrophy, detect early amnestic mild cognitive impairment. PLoS One 8 (3), e58887. https://doi.org/10.1371/journal.pone.0058887.